Combinatorial Effect of Two Framework Mutations (E119V and I222L) in the Neuraminidase Active Site of H3N2 Influenza Virus on Resistance to Oseltamivir[∇][†]

Mathilde Richard,[1]* Olivier Ferraris,[1] Alexandra Erny,[1] Mendy Barthélémy,[1] Aurélien Traversier,[1]
Murielle Sabatier,[1] Alan Hay,[2] Yi Pu Lin,[2] Rupert J. Russell,[3] and Bruno Lina[1]

*Laboratoire Virologie et Pathologie Humaine (VirPath), CNRS FRE 3011-UCBL1, Université de Lyon, Faculté de Médecine RTH Laennec,
7-11 rue Guillaume Paradin, 69372 Lyon cedex 08, France[1]; The National Institute for Medical Research, The Ridgeway,
Mill Hill, London NW7 1AA, United Kingdom[2]; and Biomedical Science Research Complex, University of
St. Andrews, North Haugh, St. Andrews, Fife KY16 9ST, United Kingdom[3]*

Neuraminidase (NA) inhibitors (NIs) are the first line of defense against influenza virus. Reverse genetics experiments allow the study of resistance mechanisms by anticipating the impacts of mutations to the virus. To look at the possibility of an increased effect on the resistance phenotype of a combination of framework mutations, known to confer resistance to oseltamivir or zanamivir, with limited effect on virus fitness, we constructed 4 viruses by reverse genetics in the A/Moscow/10/99 H3N2 background containing double mutations in their neuraminidase genes: E119D+I222L, E119V+I222L, D198N+I222L, and H274Y+I222L (N2 numbering). Among the viruses produced, the E119D+I222L mutant virus was not able to grow without bacterial NA complementation and the D198N+I222L mutant and H274Y+I222L mutant were not stable after passages in MDCK cells. The E119V+I222L mutant was stable after five passages in MDCK cells. This E119V-and-I222L combination had a combinatorial effect on oseltamivir resistance. The total NA activity of the E119V+I222L mutant was low (5% compared to that of the wild-type virus). This drop in NA activity resulted from a decreased NA quantity in the virion in comparison to that of the wild-type virus (1.4% of that of the wild type). In MDCK-SIAT1 cells, the E119V+I222L mutant virus did not present a replicative advantage over the wild-type virus, even in the presence of oseltamivir. Double mutations combining two framework mutations in the NA gene still have to be monitored, as they could induce a high level of resistance to NIs, without impairing the NA affinity. Our study allows a better understanding of the diversity of the mechanisms of resistance to NIs.

The influenza A virus presents two major surface glycoproteins: hemagglutinin (HA) and neuraminidase (NA). HA mediates virus entry into the cell by binding to terminal sialic acid (N-acetyl neuraminic acid) of cellular glycoconjugates (52). NA, through its sialidase activity, facilitates the elution of progeny virions from infected cells through the cleavage of terminal sialic acid from viral and cellular glycoconjugates (36, 44, 45).

Among the nine NA subtypes described, the crystal structures of the N9 (5, 57), N2 (58, 59), N6, and N1/N4/N8 subtypes (51) have been resolved. The NA head is a tetramer composed of four identical subunits arranged with a circular 4-fold symmetry. Each monomer contains six beta sheets composed of 4 antiparallel strands. The NA active site is located centrally on each unit and forms a pocket composed of conserved residues found in all influenza A virus NA (16). All these residues form the wall of the catalytic pocket. It includes catalytic sites (R118, D151, R152, R224, E276, R292, R371, and Y406) that interact directly with the substrate, sialic acid, and framework sites (E119, R156, W178, S179, D/N198, I222,

E227, H274, E277, N294, and E425) that interact with catalytic residues to stabilize the active site (15).

Due to its conserved structure and its essential role in viral replication, NA is an attractive antiviral target. From the crystal structures of the influenza A virus NA, potent inhibitors have been developed through rational design. Currently, two NA inhibitors (NIs) are currently used in clinical practice: oseltamivir (GS4104 [33] and its prodrug GS4071 [35]) and zanamivir (GG167 [61]). A new NI, laninamivir (Daiichi-Sankyo and Biota), has recently been approved for use in Japan. NIs are structural analogues of the predicted transition state of sialic acid binding to the NA active site (14, 56). They bind to the NA active site with a higher affinity than that of the natural substrate, block its sialidase function, and prevent the release of progeny virions from infected cells.

Resistance to NIs results from changes in the NA active site which induce a reduction of affinity for NIs. Two types of mutations are observed: mutations at catalytic sites (i.e., R292K and R152K) or at framework sites (i.e., E119V, H274Y, N294S, and D198N) (20). The effect of these mutations on resistance is NA subtype dependent and drug dependent. First, mutations at catalytic sites confer resistance, but they also induce a dramatic decrease of NA activity, an impairment of growth in vitro (65), and a reduction of infectivity, pathogenicity, and transmissibility in vivo (12, 24, 26, 27, 54). Second, mutations at framework sites induce resistance without much impairing of substrate binding, NA activity, virus replicative

capacity *in vitro* (49), and infectivity and virus transmissibility *in vivo* (11, 27, 64, 66). It has been shown previously that the combination of framework mutations may have a synergistic effect on NI susceptibility, i.e., that the combination has more of an effect than the strict addition of the two mutations does, while conserving good viral fitness. A virus possessing the mutations E119V+I222V, isolated from an immunocompromised child infected with an H3N2 virus for 1 year, induced a synergistic effect on oseltamivir resistance (8). A double mutation, H274Y+I222V, was recently observed with two patients infected with the H1N1 pandemic virus for which prophylactic treatment with oseltamivir had failed (4). Recently, with the H5N1 subtype, an H274Y+I222M mutation has been observed after oseltamivir selective pressure on MDCK cells (31). In this study, we wanted to test if other combinations of framework mutations could induce a synergistic effect on resistance to NIs without impairing the virus *in vitro* and thus could be a generalized mechanism of resistance to NIs.

To this end, we tested combinations of mutations which have not already been observed or studied using reverse genetics. We constructed mutants possessing double mutations in their NA gene by the use of the A/Moscow/10/99 H3N2 background. We previously reported a framework mutation (I222L) which induced an 18-fold decrease in oseltamivir susceptibility (49). In the present study, the I222L mutation was combined (49) with known framework mutations responsible for resistance to both or either oseltamivir or zanamivir: the E119V mutation, known to confer oseltamivir resistance in the N2 subtype (1, 3, 8, 11, 27, 34, 40, 43, 53, 63, 64), the E119D mutation, obtained *in vitro* by zanamivir selective pressure (22, 24, 40), the D198N mutation, which confers oseltamivir resistance, observed in clinic with influenza B viruses (21, 40, 55), and the H274Y mutation, the most frequently observed mutation in the N1 subtype (H1N1, including the H1N1 pandemic virus and H5N1) (1–3, 7, 23, 27, 31, 62, 63, 66).

Of the four constructed double mutants, only the E119V I222L mutant was stable in MDCK cells and induced a synergistic resistance phenotype against oseltamivir.

MATERIALS AND METHODS

Neuraminidase inhibitors. Oseltamivir carboxylate (4-*N*-acetyl-5-amino-3-(1-ethylpropoxy)-1-cyclohexane-1 carboxylic acid), the active metabolite of oseltamivir, was kindly provided by Hoffmann-La Roche, Ltd. Zanamivir (4-guanidino-Neu5Ac2en) was kindly provided by GlaxoSmithKline.

Cells. Madin-Darby canine kidney (MDCK) cells used for production of viruses were purchased from Cambrex Bioscience (ATCC, CCL34) and were maintained in serum-free medium for MDCK cells (UltraMDCK; Lonza) supplemented with 1% of L-glutamine (L-Glu) (200 mM; Lonza) and 2% of penicillin-streptomycin (PS) (10,000 U penicillin/ml, 10,000 U streptomycin/ml; Lonza).

MDCK cells used for reverse genetics were maintained in Eagle minimum essential medium with Earle's balanced salt solution without L-glutamine (EMEM; Lonza) supplemented with 1% L-Glu, 2% PS, 10% fetal bovine serum (FBS; Lonza), and 1% nonessential amino acids (NEAA) (100×; Lonza).

MDCK cells expressing human 2,6-sialyltransferase (MDCK-SIAT1) (38) were kindly provided by H.-D. Klenk (Institute of Virology, Philipps University, Marburg, Germany). They were maintained in Dulbecco's modified Eagle's medium with 4.5 g/liter glucose without L-glutamine (DMEM; Lonza) supplemented with 1% of L-Glu, 2% of PS, 10% of FBS, and 1% NEAA and under the pressure of 1 mg/ml of G-418 sulfate (Promega).

293T cells were purchased from the ATCC (CRL-11-268) and maintained in DMEM supplemented with 1% of L-Glu, 2% of PS, and 10% of FBS.

Generation of A/Moscow/10/99 H3N2 mutant viruses by reverse genetics. We used an eight-plasmid system to generate viruses in the A/Moscow/10/99 H3N2

background (28). cDNAs were cloned in the pHW2000 plasmid as already described (42). Mutations were introduced in the NA plasmid using the QuikChange site-directed mutagenesis kit (Stratagene). The nucleotide changes were the following: for E119D, E/GAA to D/GAT; for E119V, E/GAA to V/GTA; for D198N, D/GAT to N/AAT; for H274Y, H/CAT to Y/TAT; and for I222L, I/ATC to L/CTC. All the constructed plasmids were sequenced (GATC Biotech) to ensure fidelity to the strain strand and/or the presence of the desired mutations.

293T cells in coculture with MDCK cells (ratio of 70:30) were transfected by eight cDNA cloned in the pHW2000 plasmid (1 μg per plasmid) using Superfect (Qiagen) according to the manufacturer's recommendations in Opti-MEM medium (Gibco). Cells were incubated at 37°C. At 24 h posttransfection, 1 μg/ml of trypsin (Roche) was added to the culture and if necessary 2 mU/ml of NA of *Clostridium perfringens* (Sigma), and the cells were incubated at 34°C. Supernatants were harvested 72 h posttransfection, clarified of cellular remains by centrifugation at 1,800 × *g* for 5 min, and frozen at −80°C.

Passages in MDCK and MDCK-SIAT1 cells. Reverse genetics supernatants were used to infect confluent MDCK cells at 1:2 and 1:10 dilutions in EMEM, 1% L-Glu, 2% PS supplemented with 1 μg/ml of trypsin (working medium) at 34°C (the P1 passage). Viruses were harvested depending on the induced cytopathic effect (CPE). Viruses which did not induce a CPE were harvested at 96 h postinfection (p.i.). Then the last dilution (1:2 or 1:10) which induced a CPE was titrated on MDCK cells as described below and was used to infect MDCK cells at a multiplicity of infection (MOI) of 0.01. Viruses which did not induce a CPE were reinfected at a 1:2 dilution (the P2 passage) (see Table SA1 in the supplemental material). Viruses were then passaged successively in MDCK cells for three more passages at an MOI of 0.001 (the P3 to P5 passages).

Passages in MDCK-SIAT1 cells were done as described for MDCK cells. Between passages, viruses were titrated in MDCK-SIAT1 cells.

Infectious titers. Infectious titers (doses infecting 50% of the cell culture [TCID$_{50}$]/50 μl) were performed in confluent MDCK and MDCK-SIAT1 cells as previously described (42). The cytopathic effect was visible after incubation at 34°C for 96 h, and the test was revealed by hemagglutination tests performed with 0.5% chicken red blood. The number of TCID$_{50}$s/50 μl were calculated by the Reed and Muench test (48).

Plaque assays. Confluent MDCK cells were incubated 1 h at 34°C with 10-fold serial dilutions of viruses in working medium. The supernatants were then withdrawn, and the cells were overlaid by freshly prepared EMEM (2× concentrate; Lonza) containing 0.55% of agar (Agar Noble; Difco) and 1 μg/ml of trypsin. For each virus, three plaques per morphology were harvested and amplified on MDCK cells.

Reverse transcription was done after extraction of RNAs from cellular supernatants. The NA and HA genes were then specifically amplified and sequenced (GATC Biotech). Sequences were then analyzed by SeqMan software.

Kinetics in MDCK-SIAT1 cells. Confluent MDCK-SIAT1 cells were infected at an MOI of 10^{-4} in the presence or in the absence of 200 μg/ml of oseltamivir carboxylate. At the indicated times, supernatants were harvested and frozen at −80°C. Infectious titers of each collection were determined with confluent MDCK cells as described in the previous section.

Purification of viruses. P4 viruses were used to infect MDCK cells at an MOI of 10^{-4}. Viruses were concentrated through a 25% (wt/wt) sucrose cushion in phosphate-buffered saline (PBS) and then concentrated through a linear gradient of sucrose in PBS (22% [wt/wt] to 60% [wt/wt]). The final pellets were resuspended in HBS-N buffer (0.01 M HEPES, 0.15 M NaCl, pH 7.4), aliquoted, and conserved at −80°C. The amount of total viral proteins was determined using a Micro BCA protein assay kit (Thermo Scientific, Pierce) according to the manufacturer's recommendations.

Total quantification of mutant NA proteins. Total NA protein quantification was performed using an enzyme-linked immunosorbent assay (ELISA). For each purified virus, serial 2-fold dilutions were done under 50 μl/well of PBS from 0.5 μg of total viral protein and then allowed to coat a 96-well plate overnight under a wet atmosphere. After the cells were washed for 5 min three times with PBS and 0.05% Tween 20 (Sigma) at room temperature on gentle shaking (150 μl/well), plates were saturated with blocking reagent (Roche) for 1 h at 37°C under a wet atmosphere (100 μl/well). The cells were washed three times as previously described. IgG anti-A/Moscow/10/99 NA monoclonal antibody diluted at 1:1,000 in PBS and 0.05% Tween 20 (50 μl/well) was added, and contact was made for 1 h at 37°C under a wet atmosphere. Cells were washed three times as previously described. Horseradish peroxidase-conjugated sheep anti-mouse IgG (GE Healthcare) diluted at 1:1,000 in PBS and 0.05% Tween 20 (50 μl/well) was added, and plates were incubated 1 h at 37°C under a wet atmosphere. Cells were washed three times as previously described. Freshly made ABTS substrate solution (2,2′-azino-di-[3-ethylbenzthiazoline sulfonate (6)], diammonium salt crys-

tals, 1 mg/ml in ABTS buffer from Roche) (50 μl/well) was added, and contact was made for 30 min at room temperature under gentle shaking and in darkness. A lecture was done at 405 nm with a microplate reader (UMV 340 Asys; BioServ). Blank corrected data were plotted, and linear parts of the plots were used to determine the levels of NA present in each virus relative to that of the wild-type virus. To be more precise and free of the eventual cellular contamination taken into account in the protein quantification, the results were normalized against the quantity of nucleoprotein detected in virion by the same assay performed in parallel from the same 2-fold dilutions using a specific monoclonal anti-nucleoprotein antibody. The NA protein quantities are expressed as a percentage of the wild-type NA protein quantity divided by the ratio of nucleoprotein (ratio of NP is the percentage of mutant virus NP relative to the wild-type virus NP divided by 100). The anti-NA and anti-NP monoclonal antibodies were produced in the VirPath (CNRS FRE3011-UCBL1) laboratory.

Expression of NA at the surface of infected cells. P5 viruses were diluted in working medium to infect confluent MDCK 96-well plates at MOIs of 1, 1.5, and 2 (four replicates per MOI, 50 μl/well). Plates were placed for 2 h at 4°C to allow the viruses to bind to the cell surface and to allow the synchronization of the infections. Then inoculums were withdrawn and placed in freshly working medium (100 μl/well). Plates were incubated at 34°C under 5% CO_2. At 13 h postinfection, cells were fixed with formaldehyde (3.65% [in PBS], 100 μl/well). Then a saturation step was performed with blocking reagent (Roche) for 30 min at 37°C under a wet atmosphere (100 μl/well). Cells were washed three times with PBS (150 μl/well). Specific A/Moscow/10/99 NA monoclonal antibody was added at a dilution of 1:100 in PBS and 1% bovine serum albumin (BSA) (50 μl/well), and plates were incubated 1 h at 37°C under a wet atmosphere. Cells were washed three times as previously described. Fluorescein isothiocyanate (FITC)-conjugated goat anti-mouse IgG (Immunotech) was added at a dilution of 1:50 in PBS and 1% BSA (50 μl/well), and plates were incubated 1 h at 37°C under wet atmosphere. After a last step of washings, glycerol buffer (0.042% Na_2CO_3 [wt/vol], 0.386% $NaHCO_3$ [wt/vol], 90% glycerol [vol/vol] in H_2O, pH 9) was added to the wells, and fluorescent signal was read at a λ excitation of 485 nm and a λ emission of 538 nm (Dynex; MRX fluorimeter). Blank corrected data were normalized against the quantity of infected cells reflected by the relative quantity of NP expressed in the cells, determined by the same assays performed in parallel after permeabilization of the infected cells. Results were expressed as the mean of values obtained for the three MOI values and as a percentage of wild-type NA expression.

NA activity and inhibition assays. Fluorimetric NA activity assays were done as described by Ferraris et al. (19). Total NA activities were calculated as the quantity of 2′-(4-methylumbelliferyl)-α-D-N-acetylneuraminic acid (MUN) substrate degraded in 1 h per ml of viral suspensions (nmol/h/ml). Total NA activities were then expressed as a percentage of the wild-type total NA activity divided by the ratio of nucleoprotein determined by the ELISA-type assays previously described and performed in parallel from the same 2-fold dilutions. To obtain specific NA activities, total NA activities were divided by the ratio of NA protein previously determined (ratio is the percentage of mutated NA present in virion relative to that of the wild-type NA present in virion divided by 100) and were expressed as a percentage of wild-type specific NA activity.

The NA activity inhibition assay was performed as described by Ferraris et al. (19) using a standardized dose of NA activity (10 nmol/h/ml). The 50% inhibitory concentrations (IC_{50}s) of antiviral drugs were calculated according to the concentration required for reducing NA activity by 50% by analysis with Sigma Plot software.

Measurement of the Michaelis-Menten constant. The Michaelis-Menten constant (K_m), which reflects the affinity of NA for the substrate, was evaluated with viral suspensions using the MUN substrate as previously described (13, 46). The K_m was determined as the substrate concentration for which the initial velocity is at 50% of its value at substrate saturation.

RESULTS

Growth and stability of the viruses in MDCK cells. Recombinant viruses containing NAs with double mutations E119D +I222L, E119V+I222L, D198N+I222L, and H274Y+I222L were produced by reverse genetics on the H3N2 A/Moscow/10/99 background. Supernatants from reverse genetics were passaged two times in MDCK cells to determine their ability to grow *in vitro* (P1 and P2 passages).

The E119D I222L mutant virus induced no cytopathic effects

TABLE 1. Plaque characteristics of mutant viruses after the fifth passage in MDCK cells

Virus	Plaque assay after the 5th passage in MDCK cells[a]		
	Plaque size (%)[b]	NA analysis	
		K_m (μM)[c]	Mutation(s)
Wild type	L (100)	6.95 ± 0.77	—
I222L mutant	M (100)	66.30 ± 8.45	I222L
E119V mutant	M (100)	3.17 ± 0.57	E119V
E119V+I222L mutant	S (100)	14.04 ± 6.80	E119V+I222L
D198N mutant	M (100)	27.42 ± 2.61	D198N
D198N+I222L mutant[d]	M (100)	62.83 ± −2.23	I222L
H274Y mutant	M (100)	30.33 ± 1.38	H274Y
H274Y+I222L mutant[e]	M (100)	37.90 ± 2.39	H274Y

[a] Plaque assays were performed with MDCK cells after the fifth passage in MDCK cells. For each virus, three clones per morphology were picked and amplified in MDCK cells. The HA and NA genes of the three clones were sequenced. No mutations were found in the HA genes of any viral clones. —, no mutations.

[b] Plaque sizes: L, large plaque (from 2 to 2.5 mm); M, medium plaque (from 1 to 1.5 mm); S, small plaque (from 0.5 to 1 mm). Numbers in parentheses correspond to the proportion of large, medium, and small plaques.

[c] K_m values are expressed as the mean ± standard deviation of the values from the three clones determined from two independent assays.

[d] At the third passage, all the plaques had the same morphology (M) and the NA gene contained the only I222L mutation. At the first passage, all the plaques had the same morphology (S) and the D198N+I222L mutations were detected in the NA gene.

[e] At both first and third passages, all the plaques had the same morphology (M) and the H274Y mutation was detected in the NA gene.

in MDCK cells and was not detectable by hemagglutination tests (<2 hemagglutination units [HAU]/50 μl). To confirm these observations, we performed two other reverse genetics experiments, and the same results were observed. However, the E119D+I222L mutant was able to grow in the presence of 2 mU/ml of NA of *Clostridium perfringens*, suggesting that the defect in growth is due only to a deficiency in the total NA activity of the mutant virus. This virus was not further investigated because of its inability to grow in MDCK cells without bacterial NA activity complementation.

The E119V+I222L and H274Y+I222L mutant viruses induced a cytopathic effect in MDCK cells and were detectable by hemagglutination assays at the first passage. The D198N+I222L mutant was detectable by hemagglutination assays only at the second passage, but it induced a cytopathic effect in MDCK cells at the first passage. To further investigate the stability of the E119V+I222L, D198N+I222L, and H274Y+I222L viruses, three additional passages were performed in MDCK cells (the P3 to P5 passages). As references, the I222L, E119V, D198N, and H274Y single mutants were produced and passaged five times in MDCK cells under the same conditions as those of the wild-type virus. After the fifth passage, plaque assays with MDCK cells were done. All the viruses presented homogenous plaque morphology and thus a homogenous population. Three clones per virus were picked. Viral RNAs were then extracted, and NA and HA genes were amplified and sequenced (Table 1).

All the viruses presented plaque morphologies different from that of the wild-type virus. Three plaque morphologies were observed: large plaques (2 to 2.5 mm), medium plaques

(1 to 1.5 mm), and small plaques (0.5 mm). Large plaques were observed only for the wild-type virus.

The only double mutant stable after five passages in MDCK cells was the E119V+I222L mutant. The D198N+I222L and H274Y+I222L viruses reverted toward a single mutant. Interestingly they did not revert toward the same single mutant. The D198N+I222L virus conserved the I222L mutation, and the H274Y+I222L mutant the H274Y mutation. To understand when the reversions took place, we performed plaque assays with MDCK cells with the D198N+I222L and H274Y+I222L viruses resulting from the third and the first passages. The H274Y+I222L virus had already reverted at the first passage in MDCK cells. The D198N+I222L virus had reverted at the third passage in MDCK cells, but the virus still presented the double mutation at the first passage during which it was rescued, i.e., the second passage in MDCK cells.

To investigate if the conservation of the double mutation E119V+I222L after the fifth passage was accompanied by mutations in the HA gene, counterbalancing eventual defects generated by the mutations in the NA active site, the HA gene of the E119V+I222L mutant was sequenced. No mutations were found, implying that the double mutation in the NA was maintained without the need of modifications in the HA. The HA genes of all other viruses, the wild type, single mutant, and reverted mutants, were also sequenced, and no additional mutations were found.

These genetic characteristics were confirmed by phenotypic observations. The E119V+I222L mutant presented a small-plaque phenotype, different from those of the wild-type, E119V, and I222L viruses. The plaque morphology of all reverted mutants corresponded to the plaque morphology of the virus to which they reverted. The Michaelis-Menten constant (K_m), which indicates the affinity of the NA for its substrate and which is an intrinsic characteristic of the protein, was measured for each clone by fluorimetric assays using a 2′-(4-methylumbelliferyl)-α-D-N-acetylneuraminic acid substrate. The E119V+I222L mutant had a K_m value which was different from the wild-type, the E119V mutant, and the I222L mutant K_ms. All the reverted mutants presented the same K_m as that of the virus to which they had reverted.

The I222L mutation induced a 9.5-fold decrease in NA affinity (K_m), and the E119V mutation induced a 2-fold increase in NA affinity. The combination of these two mutations induced only a slight decrease, with a factor of 2, compared to the wild-type NA affinity. This decrease of NA affinity was the smallest among those for all single mutations tested, apart from that for the E119V mutation.

No more investigations were done with the D198N+I222L and H274Y+I222L viruses, as they were not stable in MDCK cells and as these mutations may not have a clinical interest. However, the E119V+I222L double mutant was further analyzed in parallel with the E119V and I222L single mutants and the wild-type virus.

Virological characteristics of the E119V+I222L mutant. (i) NA inhibition assays. The aim of this study was to study the effects of combinations of single NA mutations on NI resistance. To assay if the only stable double mutation that we obtained induces a synergistic effect in the phenotype of resistance to either or both NIs, oseltamivir and zanamivir, we measured NI concentrations which inhibit 50% of the NA

TABLE 2. Concentrations of NIs inhibiting 50% of the NA activity (IC$_{50}$)

Virus	NI IC$_{50}$ (nM)[a]	
	Oseltamivir	Zanamivir
Wild type	0.37 ± 0.03	2.90 ± 0.38
I222L mutant	3.26 ± 0.08 (9)***	6.05 ± 0.28 (2)***
E119V mutant	72.82 ± 6.18 (197)***	3.07 ± 0.25 (1)
E119V I222L mutant	581.33 ± 58.09 (1,571)***###¤¤¤	14.78 ± 1.34 (5)***###¤¤

[a] Mean IC$_{50}$ ± standard deviation calculated using values derived from three separate assays performed in duplicate. Numbers in parentheses correspond to the fold differences in the IC$_{50}$ with the wild-type virus. The results were analyzed by a two-tailed Welch t test using R software. ***, P value < 0.0005, t test against the A/Moscow/10/99; ###, P value < 0.0005, t test against the I222L virus; ¤¤¤, P value < 0.0005, t test against the E119V virus.

activity (IC$_{50}$) for the viruses purified after the fifth passage in MDCK cells (Table 2).

The E119V+I222L mutant was found to be 1,571 times more resistant to oseltamivir than the wild type was, whereas the E119V mutation induced a moderate resistance (197-fold) and the I222L mutation induced a slight resistance (9-fold). The combination of two mutations which induce moderate resistance to oseltamivir led to a synergistic effect and a strong phenotype of resistance, which was statistically different from those of the wild-type, I222L mutant, and E119V mutant phenotypes.

This synergistic effect was not observed for zanamivir resistance. The double mutant induced only a 5-fold decrease in the zanamivir IC$_{50}$, the I222L virus induced a 2-fold decrease, and the E119V virus did not have a significant difference in the zanamivir IC$_{50}$ compared to that of the wild-type virus.

(ii) Total NA activity. The E119V I222L double mutant induced high resistance to oseltamivir. As changes in the NA active site may cause a reduction in NA activity, we assayed the total NA activity of the double mutant. NA activity tests were performed on viruses purified after the fifth passage in MDCK cells. We measured total NA activity by fluorimetric tests using a MUN substrate. Activities were normalized against the quantity of nucleoprotein as described in Materials and Methods. Normalization against the quantity of NP is an indirect means of normalizing against the number of viral particles (as the quantity of NP may not vary in each particle), and our results reflect the total NA activity of each viral particle (Fig. 1A).

The I222L and E119V viruses had total NA activities which represented 75.5% and 24.4% of that of the wild type, respectively. The E119V+I222L double mutant showed very low total NA activity, with only 5% of that of the wild type.

(iii) Quantification of NA protein in virions. To understand if this large drop in total NA activity for the double mutant is due to a disruption of the intrinsic NA activity caused by the changes in the NA active site or to a drop in the quantity of NA protein in the virus, we developed an ELISA-based assay to quantify the mutant NAs in virions relative to the quantity of wild-type NA. The detection of NA was performed using a specific monoclonal antibody directed against A/Moscow/10/99 NA, as described in Materials and Methods, on the purified viruses after the fifth passage in MDCK cells. The results were normalized against the quantity of nucleoprotein as described
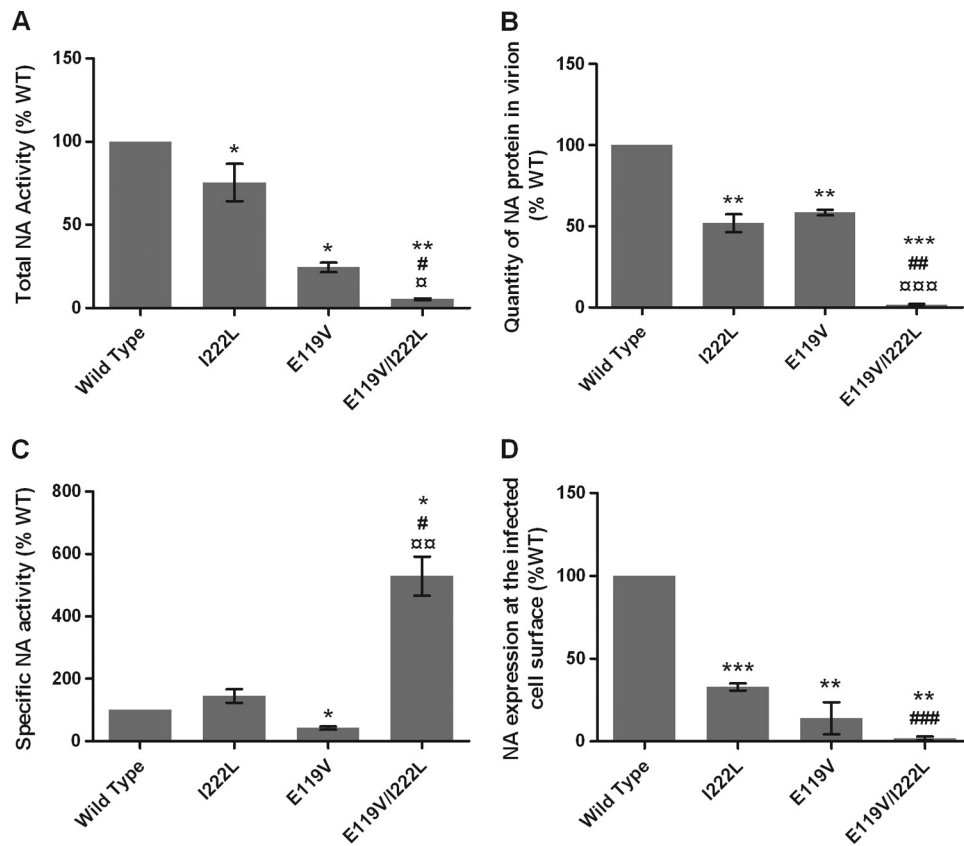
FIG. 1. NA characteristics of the wild-type (WT), I222L, E119V, and E119V+I222L viruses. NA characteristics of the I222L, E119V, and E119V+I222L viruses were expressed as a percentage of that of the wild-type virus, always expressed as 100%. (A) Total NA activity of I222L, E119V, and E119V+I222L viruses relative to that of the wild-type virus determined by fluorimetric assays using MUN as substrate. Results are expressed as a percentage of the wild-type value. Mean values ± standard deviation calculated from three independent assays. (B) Total NA quantity in I222L, E119V, and E119V+I222L viruses relative to that in the wild-type virus determined with an ELISA-based assay using a monoclonal antibody directed against the NA of A/Moscow/10/99. Results are expressed as a percentage of the wild-type value. Mean values ± standard deviation calculated from three independent assays. (C) Specific NA activity of I222L, E119V, and E119V+I222L viruses relative to that of the wild-type virus determined by the ratio of the total NA activity on the total quantity of NA. Results are expressed as a percentage of the wild-type value. Mean values ± standard deviation calculated from three independent assays. (D) Expression of the I222L, E119V, and E119V+I222L virus NAs at the infected cell surface. Results are expressed as a percentage of the wild-type values for the three MOI mean values ± standard deviation calculated from three independent assays. The results were analyzed by a two-tailed Welch *t* test using R software. ∗, *P* value < 0.05; ∗∗, *P* value < 0.005; ∗∗∗, *P* value < 0.0005, against the A/Moscow/10/99. #, *P* value < 0.05; ##, *P* value < 0.005; ###, *P* value < 0.0005, *t* test against the I222L virus. ¤, *P* value < 0.05; ¤¤, *P* value < 0.005; ¤¤¤, *P* value < 0.0005, *t* test against the E119V virus.

in Materials and Methods and reflect the quantity of mutated NA in virion (Fig. 1B).

The I222L and E119V mutations reduced the total quantity of NA in virion by 48.2% and 41.5%, respectively, compared to that of wild-type NA. The double mutant NA was present in virion at only 1.4% of that of wild-type NA.

(iv) Specific NA activity. Total NA activities were divided by the quantity of NA present in virion to obtain specific NA activity (Fig. 1C). The E119V virus NA had a specific activity of 42.1% of that of the wild-type NA. This mutation seems to affect both the quantity of NA in the virion and NA activity itself. As the I222L virus NA was expressed only at 51.8% of that of the wild type but still had a great activity, its specific activity was, under these conditions, similar to that of the wild-type virus. For the double mutant, the NA activity itself was not impaired, as under these conditions the specific NA activity was 5.3 times higher than that of the wild type. The fact that the double mutant has a low total NA activity is due only

to its low quantity in virion, but the double mutation does not affect the intrinsic NA activity.

(v) Expression of the mutant NA at the infected cell surface. To understand if the reduction of the amount of mutant NA in virion was due to a reduction of incorporation of the protein into the virion during the budding process or of the quantity of the protein at the infected cell surface, we performed an assay to quantify the NA present at the infected cell surface. Briefly, P5 viruses were used to infect MDCK cells at an MOI of 1, 1.5, and 2. At 13 h postinfection, an immunofluorescent assay was performed without permeabilizing the cell surface of the infected cells (Fig. 1D). To control if the infected cell membrane was not effectively permeabilized, the NP was detected by the same assay. No signal was detected. The results were normalized against the quantity of infected cells as described in Materials and Methods.

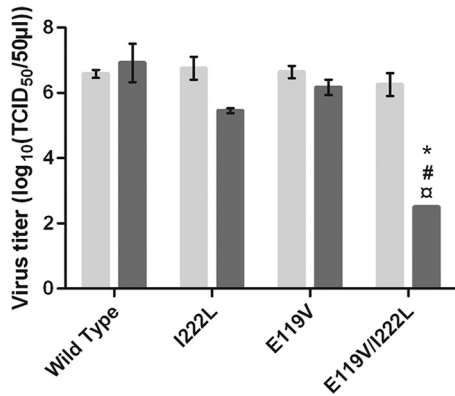For the I222L and E119V viruses, the total NA quantity at the infected cell surface corresponded to 33% and 14% of

FIG. 2. Infectious titers in MDCK and MDCK-SIAT1 cells. Viruses were titrated after the fifth passage in MDCK cells (light gray) and in MDCK-SIAT1 cells (dark gray). Mean values ± standard deviation are from two independent assays. The results were analyzed by a two-tailed Welch t test using R software. $*$, P value < 0.05, against the A/Moscow/10/99. $\#$, P value < 0.05, t test against the I222L virus. ϖ, P value < 0.05, t test against the E119V virus.

the wild-type NA quantity, respectively. The double mutant NA was hardly detectable (2.1% compared to that of the wild-type NA).

The levels of mutant NA quantity at the cell surface are different for the mutant viruses and for the wild-type virus, implying that the incorporation in the virion is probably not affected by the NA mutations. Further investigations are needed to understand precisely which stage of the protein processing the mutations impaired.

(vi) Replicative capacity in MDCK and MDCK-SIAT1 cells. To assay the effect of the E119V+I222L mutation on the growth characteristics of the virus, we determined infectious titers ($TCID_{50}/50$ µl) in MDCK cells and in MDCK-SIAT1 cells after the P5 passage (Fig. 2). MDCK-SIAT1 cells overexpress sialic acid in conformation α2,6 with the last sugar, galactose (for the sake of the brevity, referred to as SAα2,6Gal). As human HAs show greater affinity for SAα2,6Gal, viruses are more dependent on the NA activity to elute from MDCK-SIAT1 cells than from MDCK cells.

No significant differences in infectious titers in MDCK cells between mutant and wild-type viruses were observed. This implies that the mutations studied did not have any effect on the growth characteristics of the viruses in MDCK cells, even if some strongly decreased the total NA activity of the virus.

In MDCK-SIAT1 cells, the E119V+I222L virus was the only one to present a significant drop in replicative capacity compared to MDCK cells (P value = 0.043). The 4-log decrease in replicative capacity, in comparison to that of the wild type, observed for the E119V+I222L virus was due to its low total NA activity.

(vii) Oseltamivir resistance in cellular models: kinetics in MDCK-SIAT1 cells. To integrate other parameters in the determination of the phenotype of resistance, as NA activity and replicative capacity *in vitro*, we wanted to assay the resistance of the E119V+I222L virus in a cellular context. We did kinetics experiments with MDCK-SIAT1 cells. Briefly, a 0.0001 MOI was used to infect confluent MDCK-SIAT1 cells in the absence or in the presence of 200 µg/ml of oseltamivir. Supernatants were harvested at different time points, and the $TCID_{50}/50$ µl was determined in MDCK cells (Fig. 3A and B).

In the absence of oseltamivir, the I222L and E119V viruses, which presented a total NA activity of about 75% and 24% of that of the wild type, respectively, showed a 1-log to 1.5-log decrease in the $TCID_{50}/50$ µl throughout the kinetics. The E119V+I222L mutant was greatly impaired and showed a large deficit of replicative capacity (an about 3-log decrease throughout the kinetics).

In the presence of oseltamivir, the wild-type virus showed a 3-log decrease at 96 h p.i., the I222L virus a 1.5-log decrease, and the E119V a 2.5-log decrease. The E119V+I222L virus was the only one to maintain its replicative capacity in the presence of 200 µg/ml of oseltamivir, confirming the phenotype of resistance induced by the double mutation E119V+I222L. However, as its replicative capacity was impaired in MDCK-SIAT1, its maintenance in the presence of oseltamivir is not sufficient to allow the mutant to replicate better than the wild-type virus under selective pressure. The drop in total NA activity of the E119V+I222L virus reduced
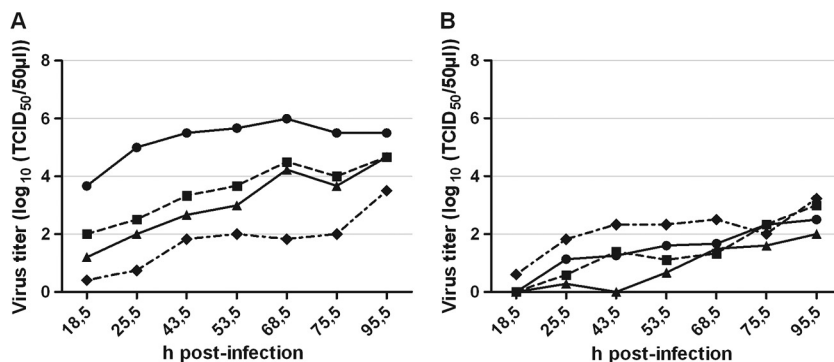

FIG. 3. Kinetics in MDCK-SIAT1 in the absence or in the presence of oseltamivir. (A) The viruses were produced by reverse genetics and passaged five times on MDCK cells. Each P5 virus was used at an MOI of 0.0001 to infect MDCK-SIAT1 cells in the presence of trypsin (1 µg/ml). At the indicated time points, supernatants were harvested, and virus titers ($TCID_{50}/50$ µl) were determined with MDCK cells for each virus: wild type (circle), I222L mutant (square), E119V mutant (triangle), and E119V+I222L mutant (diamond). (B) Kinetics was performed under the same conditions as those described for panel A, in the presence of 200 µg/ml of oseltamivir.
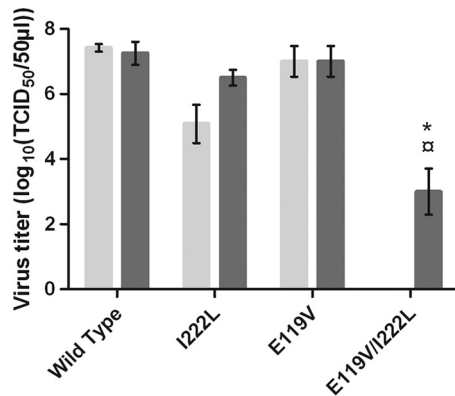
FIG. 4. Infectious titers in MDCK-SIAT cells after the third and the fifth passages in MDCK-SIAT1 cells. The wild-type, I222L, E119V, and E119V+I222L viruses were passaged five times in MDCK-SIAT1 cells, and infectious titers in MDCK-SIAT1 cells were determined after the third (light gray) and the fifth (dark gray) passages. Mean values ± standard deviation are from two independent assays. The results were analyzed by a two-tailed Welch t test using R software. ∗, P value < 0.05, against the A/Moscow/10/99. ¤, P value < 0.05, t test against the E119V virus.

the advantage conferred by a resistance phenotype in cellular models.

(viii) Stability in MDCK-SIAT1 cells. The combination of the E119V+I222L mutations was the only one stable in MDCK cells. However, the replicative capacity of the E119V+I222L virus in MDCK-SIAT1 cells was impaired due to its low total NA activity. As the NA is under greater selective pressure in MDCK-SIAT1 cells than in MDCK cells, we wanted to test the genetic stability of the double mutant in MDCK-SIAT1 cells. The wild-type virus and the I222L, E119V, and E119V+I222L viruses were passaged five times in MDCK-SIAT1 cells under the same conditions as the five passages done in MDCK cells (except for the double mutant which was passaged at a dilution of 1:2 for each passage).

The infectious titers of all the viruses after the third and the fifth passages are presented in Fig. 4. Both the I222L and E119V viruses showed infectious titers at the third and fifth passages not significantly different from those of the wild-type virus. However, the double mutant was not able to grow efficiently in MDCK-SIAT1 cells. For the first four passages, a CPE was visible on the cells, but no viruses were detectable by phenotypic tests (hemagglutination titer of <2 HAU/50 μl and a TCID$_{50}$/50 μl of <1). At the fifth passage, the virus was detectable, but its infectious titer was very low (10^3 TCID$_{50}$/50 μl). As expected, the weak total NA activity of the E119V+I222L mutant was more prejudicial for the growth of the virus in MDCK-SIAT1 than in MDCK cells.

After the fifth passage in MDCK-SIAT1 cells, plaque assays with MDCK cells were performed to assay the genetic stability of the double mutant (Table 3). The wild-type virus and the E119V and I222L viruses presented homogenous plaque morphology (large and medium plaques, respectively), but the E119V+I222L virus presented a mix of small (81%) and large (19%) plaques. For each virus, three clones per morphology were picked and amplified in MDCK cells. NA and HA genes

were sequenced, and Michaelis-Menten constants were determined.

The wild-type virus and the E119V and I222L clones presented the same plaque morphologies, K_m values, and NA genotypes as the clones produced in MDCK cells. A fifth of the clones of the E119V+I222L double mutant had their plaque morphologies changed from the small phenotype observed with MDCK cells to the medium phenotype. The mean K_m values of three clones in the medium population were similar to the K_m values of E119V viruses, and their sequencing revealed a reversion to the E119V mutation. The other four-fifths had conserved their small phenotypes, their K_m values were similar to that of the E119V+I222L virus in MDCK cells, and sequencing of three clones revealed the presence of the double mutation E119V+I222L. The double mutant is more impaired and less stable in MDCK-SIAT1 cells than in MDCK cells due to its weak total NA activity. HA genes of each clone for the wild-type, I222L, E119V, and E119V+I222L viruses were sequenced, and no compensatory mutations were detected.

DISCUSSION

The hypothesis of this study was that a combination of framework mutations, known to confer moderate resistance to either or both NIs without impairing the virus, may have a synergistic effect on NI resistance without a negative impact on viral fitness. To test this hypothesis, we constructed viruses in the A/Moscow/10/99 H3N2 background containing double mutations in their NA active sites. All mutations were in combination with the I222L mutation that we found in a previous study. This mutation is responsible for an 18-fold decrease of oseltamivir susceptibility in NA inhibition assays (49).

Among the 4 double mutants that we produced, one did not grow in MDCK cells (the E119D+I222L mutant), and two were not stable in MDCK cells and reverted at the first or the second passage in MDCK cells (the D198N+I222L and

TABLE 3. Plaque characteristics of the mutant viruses after five passages in MDCK-SIAT1 cells

Virus	Plaque assay after the 5th passage in MDCK-SIAT1 cells[a]		
	Plaque size (%)[b]	NA analysis	
		K_m (μM)[c]	Mutation(s)
Wild-type virus	L (100)	8.63 ± 1.52	
I222L mutant	M (100)	62.07 ± 10.36	I222L
E119V mutant	M (100)	2.99 ± 1.39	E119V
E119V+I222L mutant	S (81)	19.82 ± 0.41	E119V+I222L
	M (19)	2.04 ± 0.58	E119V

[a] Plaque assays were performed with MDCK cells after the fifth passage in MDCK-SIAT1 cells. For each virus, three clones per morphology were picked and amplified in MDCK cells. The NA and HA genes of the three clones were sequenced. No mutations were detected in the HA genes of any of the four viruses.

[b] Plaque sizes: L, large plaque (from 2 to 2.5 mm); M, medium plaque (from 1 to 1.5 mm); S, small plaque (from 0.5 to 1 mm). Numbers in parentheses correspond to the proportion of large, medium, and small plaques.

[c] K_m values are expressed as the mean ± standard deviation of the values from the three clones determined from two independent assays.

H274Y+I222L mutants). Only one virus was stable in MDCK cells (the E119V+I222L mutant).

However, we observed that the E119D+I222L mutant, which was not able to grow for the first two passages in MDCK cells, retrieved its growth ability by the bacterial NA complementation. This reflects defective NA activity. Interestingly, an aspartic acid in position 119 is detrimental, when combined with the I222L mutation, whereas a valine at this position is not. An aspartic acid at position 119 might cause R118 to shift in order to interact electrostatically with its carboxylic group. Thus, R118 would be forced to move away from the catalytic site where it normally interacts with the carboxylate group of sialic acid, affecting presumably sialic acid binding. The flexibility of R118 has been observed recently with crystallographic structures of the N1 active site in complex with sialic acid derivatives (50). As valine is hydrophobic, its presence would not disturb the interaction of R118 with sialic acid.

Regarding the D198N+I222L and H274Y+I222L viruses that reverted toward a single mutant, structural data show that the D198 and H274 residues are close to the I222 residue. Hence, mutations at both the D198 and I222 and the H274 and I222 sites may cause a bigger structural change than in single mutants. In contrast, the E119 and I222 residues affect different parts of the active site, and mutations at these sites have less chance to disturb the NA active site, explaining why the E119V+I222L virus can be stable.

Interestingly, the two D198N+I222L and H274Y+I222L double mutants reverted to different single mutations: the D198N+I222L mutant conserved its I222L mutation and the H274Y+I222L virus its H274Y mutation. This differential reversion could be analyzed in terms of which mutation is less prejudicial for the virus. No viruses reverted to the wild-type virus, suggesting that the loss of two mutations may be more costly than the eventual impairment due to a single mutation. However, we performed this experiment only once, so we cannot conclude about the profile of reversion. The fact that these viruses have reverted once *in vitro* allows us to predict that they might not be stable *in vivo*.

This study showed that the combination between the two framework mutations E119V and I222L, known to confer moderate resistance to oseltamivir, are synergistic in the oseltamivir resistance phenotype. The E119V+I222L mutation increased the oseltamivir resistance conferred by the I222L and the E119V mutations by 179 times and 8 times, respectively. The double mutant was *in fine* 1,570 times more resistant than the wild-type virus.

The E119 residue is conserved among all influenza A viruses and forms a hydrogen bond with the hydroxyl group on the C-4 of sialic acid (60) and with the amino group on C-4 of oseltamivir (33). A lot of substitutions (E119A/D/G/I/V) have been observed *in vivo* and *in vitro*, with N1, N2, and B subtypes conferring resistance to either oseltamivir or zanamivir (2, 3, 24, 27, 31, 32, 34, 40, 43, 49, 53, 55, 63, 66). The I222 residue is a conserved residue in the NA active site whose side chain forms with W178 a hydrophobic pocket in which lies the methyl group of the acetamido group of the sialic acid and oseltamivir (60). To our knowledge, five types of substitutions have been observed *in vivo* and/or studied *in vitro* (I222V/M/L/R/T), with the N1, N2, and B backgrounds conferring moderate resistance to oseltamivir (4, 8, 25, 31, 41, 49). As the

mutations E119V+I222L affect different parts of the NA active site and inhibitor binding, their mode of action in resistance is different and their effects are additional.

A synergistic effect on the NI resistance phenotype has already been observed *in vivo* with an H3N2 virus isolated from an immunocompromised child treated with oseltamivir for 1 year. The IC_{50} of the E119V+I222V double mutant was 1,000 times higher than that of the wild-type virus. Using transfection assays, the E119V+I222V mutation conferred 293-, 152,- and 2-fold-increased IC_{50}s compared to those of the wild-type virus and the I222V and the E119V mutants, respectively (8). This was confirmed by reverse genetics experiments (11). Recently, a pandemic H1N1 (2009) virus that presented the combination of two framework mutations, H274Y+I222V, has been observed with a patient (4). Hurt et al. also observed the emergence of the H274Y+I222M double mutants of H5N1 virus selected *in vitro* by oseltamivir pressure (31). This double mutation was then produced by reverse genetics in an H1N1 background and with NAs of H5N1 and H1N1 viruses. This combination yielded an increase in oseltamivir resistance in comparison to that of the H274Y and I222M single mutants. A synergistic pattern was also reported with an H274Y+I222V combination (31), with levels of synergistic effect depending on the mutations and virus subtype. We can note that residue 222 is frequently reported for combinations of framework mutations.

The E119V+I222L mutant showed only a slight decrease in zanamivir susceptibility (5-fold), as reported for the H274Y+I222M and H274Y+I222V mutants of the H5N1 and H1N1 subtypes (31). The E119V, I222L/M, and H274Y single mutations are not responsible for resistance to zanamivir. Zanamivir is the NI with the structure closest to that of sialic acid. Hence, mutations which induce resistance to zanamivir are more likely to decrease affinity of the NA active site for sialic acid than for other NIs.

In our study, the double mutant harbored the E119V NA mutation, which was found to be 2-fold more active for the MUN substrate. However, the double mutant showed a 2-fold decrease of NA affinity. Even if reduced, this affinity was higher than that for every single mutant tested. Interestingly, the combination of framework mutations (E119V+I222L) allowed the decrease of NA active site affinity for oseltamivir (not directly measured but supposed because of the IC_{50} of 581 nM) without impairing it for the sialic acid. This could be due to the fact that isoleucine is able to orient itself such that the shorter branch of its side chain is able to pack against the pentyl ester group of oseltamivir. However, a leucine at position 222, which is uniform in length, may disrupt the optimal position of oseltamivir in this hydrophobic pocket, in a manner analogous to that observed with the common H274Y mutation. Binding to sialic acid would not be impaired, as its glycerol group is more distant from the residue in position 222 (Fig. 5).

As opposed to the double mutants described by Baz et al. and Hurt et al., the total NA activity of the E119V+I222L mutant was very low compared to that of the wild-type virus (8, 31). Indeed, the recombinant E119V+I222V NA constructed by Baz et al. retained good NA activity (72% of that of the wild type) (8). The H274Y+I222M and H274Y+I222V mutants constructed by Hurt et al. showed different levels of total NA activity, but the levels were always superior to that of the
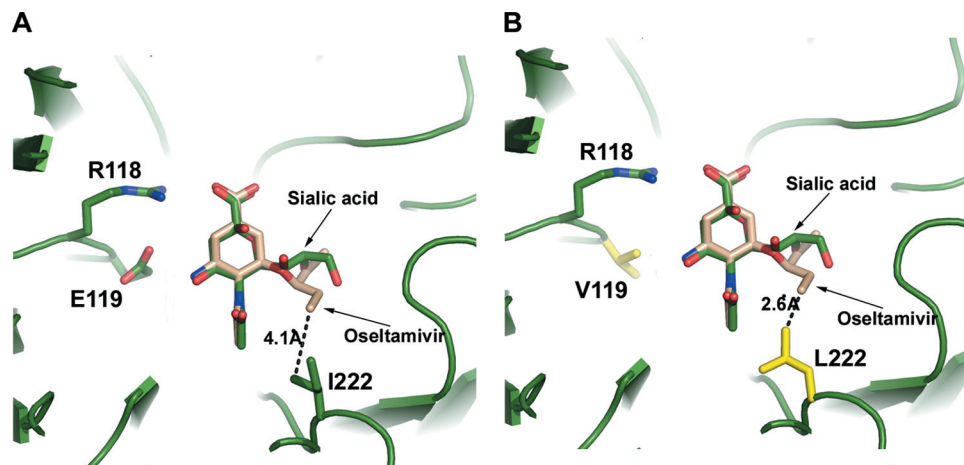
FIG. 5. Hypotheses about the differential affinities of E119V+I222L mutant NA for sialic acid and oseltamivir. (A) Schematic representation of the active site of N2 NA with sialic acid bound. The corresponding position of oseltamivir is shown in gold. (B) Model of the E119V+I222L double mutant of N2 NA, with the mutations highlighted in yellow. The figure was created using PyMOL.

E119V+I222L mutant (31). Although the methods used were not identical, E119V+I222L mutations significantly impaired the NA activity. The low NA activity of the E119V+I222L mutant resulted from a low NA quantity at the surface of the virion. The specific activity of the NA protein was not affected; it was even 5 times higher than that of the wild-type virus. This low NA quantity in the virion was a consequence of the low quantity of the mutated NA at the infected cell surface. Additional studies are needed to understand by which mechanism the double mutation E119V+I222L decreases drastically the expression of the protein at the infected cell surface: decreased mRNA transcription or protein translation, or affected protein folding or stability.

In vitro, the E119V+I222L virus replicated at the same levels as those of the wild-type virus in MDCK cells but not in MDCK-SIAT1 cells. MDCK cells possess a mix of SAα2,6Gal and SAα2,3Gal at their surface, and viruses with a low NA activity are able to replicate; the decrease in HA affinity for SAα2,3Gal is counterbalancing the defect in NA activity. As MDCK-SIAT1 cells overexpress SAα2,6Gal, viruses are more dependent on NA activity. The discrepancy between replicative abilities of the double mutant in MDCK and MDCK-SIAT1 cells may be linked to its low total NA activity. Not surprisingly, the E119V+I222L double mutant was not able to grow efficiently when passaged in MDCK-SIAT1 cells. The virus was detectable only at the fifth passage, in which a fifth of the population had reverted toward the E119V mutation. The instability of the double mutation was certainly due to an increase of pressure on NA in this cellular model.

The oseltamivir phenotype of resistance of the E119V+I222L double mutant was confirmed by kinetics experiments with MDCK-SIAT1 cells. Unlike the wild-type and the I222L and the E119V viruses, the double mutant showed no differences in growing in the presence of oseltamivir. However, as a result of its low replicative capacity in MDCK-SIAT1 cells, the double mutant lost its advantage conferred by the double mutation and did not in the presence of oseltamivir demonstrate better replication than the wild-type virus.

We can predict a low impact of this double mutant *in vivo*.

First, its lack of stability in MDCK-SIAT1 cells predicts minor chances for the double mutation E119V+I222L to be maintained *in vivo*. Second, with the observed inefficiency to infect MDCK-SIAT1 cells, which is the most reliable cellular model to study human influenza virus infections, the double mutant might have no replicative advantage over the wild-type virus *in vivo*, even in the presence of a selective pressure. However, the very similar E119V+I222V double mutant in the Panama H3N2 background was able to infect and to be transmitted in the guinea pig, which is known to be susceptible to human viruses (i.e., unadapted) (37). This discrepancy between our prediction and these results may be due just to NA activity levels. Bouvier et al. did not determine the NA activity of their double mutant (11), but Baz et al. found the well-conserved NA activity of the E119V+I222V recombinant protein (72% of the wild type) (8).

In this study, we wanted to test if a combination of framework mutations could be a generalized mechanism of resistance to NIs. We observed that, among four double mutants produced, only one was stable in MDCK cells, implying that resistant double mutations might have a low risk of emergence in the clinic. However, since there is good conservation of the substrate affinity and specific activity of the E119V+I222L mutant NA and the synergistic NI resistance phenotype, the appearance *in vivo* of double mutations in the NA active site must continue to be monitored. As double mutations have already been observed *in vivo* (4, 8) and under selective pressure (31), a combination of framework mutations may have under particular circumstances selective value over the wild-type virus, and their impact *in vivo* must not be underestimated.

Our results are a continuation of the paradigm which implies that mutations in the NA active site may have a low impact *in vivo*, as they are too deleterious for the virus. Indeed, from 1999 to 2007, the impact of resistance to NIs was very low (<0.5%) (18, 29, 41, 53). However, resistance to oseltamivir in the H1N1 subtype rose to 12 to 20% in 2007 to 2008 (17, 30, 39) and to about 100% in 2008 to 2009 (6). All the resistant H1N1 viruses possessed the H274Y mutation in the NA gene product, which seemed not to impair the fitness of the virus.

The worldwide circulation and transmission of resistant viruses were not a result of selective pressure by antivirals. Recent studies have been carried out to understand the conserved fitness of the H274Y H1N1 viruses from 2007 to 2008 (9, 10, 13, 47). These studies report the presence of mutations in the NA gene, which may allow NA to accommodate the H274Y mutation. Some of these mutations have been shown to restore H274Y NA expression at the cell surface (10). The deleterious character of our double mutant was due only to the low level of expression of the doubly mutated NA at the infected cell surface. This loss of expression may be due to a loss in protein stability or protein folding which could be restored by secondary mutations, as in H1N1 Brisbane-like H274Y viruses. For now, it would be important not only to focus on isolated mutations which confer NI resistance but also to monitor the possible adaptations of the virus to accommodate these mutations.

ACKNOWLEDGMENTS

REFERENCES

1. **Abed, Y., M. Baz, and G. Boivin.** 2006. Impact of neuraminidase mutations conferring influenza resistance to neuraminidase inhibitors in the N1 and N2 genetic backgrounds. Antivir. Ther. **11:**971–976.
2. **Abed, Y., N. Goyette, and G. Boivin.** 2004. A reverse genetics study of resistance to neuraminidase inhibitors in an influenza A/H1N1 virus. Antivir. Ther. **9:**577–581.
3. **Abed, Y., B. Nehme, M. Baz, and G. Boivin.** 2008. Activity of the neuraminidase inhibitor A-315675 against oseltamivir-resistant influenza neuraminidases of N1 and N2 subtypes. Antiviral Res. **77:**163–166.
4. **Anonymous.** 2009. Oseltamivir-resistant 2009 pandemic influenza A (H1N1) virus infection in two summer campers receiving prophylaxis—North Carolina, 2009. MMWR Morb. Mortal. Wkly. Rep. **58:**969–972.
5. **Baker, A. T., J. N. Varghese, W. G. Laver, G. M. Air, and P. M. Colman.** 1987. Three-dimensional structure of neuraminidase of subtype N9 from an avian influenza virus. Proteins **2:**111–117.
6. **Baranovich, T., et al.** 2010. Emergence of H274Y oseltamivir-resistant A(H1N1) influenza viruses in Japan during the 2008-2009 season. J. Clin. Virol. **47:**23–28.
7. **Baz, M., Y. Abed, and G. Boivin.** 2007. Characterization of drug-resistant recombinant influenza A/H1N1 viruses selected in vitro with peramivir and zanamivir. Antiviral Res. **74:**159–162.
8. **Baz, M., Y. Abed, J. McDonald, and G. Boivin.** 2006. Characterization of multidrug-resistant influenza A/H3N2 viruses shed during 1 year by an immunocompromised child. Clin. Infect. Dis. **43:**1555–1561.
9. **Baz, M., Y. Abed, P. Simon, M. E. Hamelin, and G. Boivin.** 2010. Effect of the neuraminidase mutation H274Y conferring resistance to oseltamivir on the replicative capacity and virulence of old and recent human influenza A(H1N1) viruses. J. Infect. Dis. **201:**740–745.
10. **Bloom, J. D., L. I. Gong, and D. Baltimore.** 2010. Permissive secondary mutations enable the evolution of influenza oseltamivir resistance. Science **328:**1272–1275.
11. **Bouvier, N. M., A. C. Lowen, and P. Palese.** 2008. Oseltamivir-resistant influenza A viruses are transmitted efficiently among guinea pigs by direct contact but not by aerosol. J. Virol. **82:**10052–10058.
12. **Carr, J., et al.** 2002. Influenza virus carrying neuraminidase with reduced sensitivity to oseltamivir carboxylate has altered properties in vitro and is compromised for infectivity and replicative ability in vivo. Antiviral Res. **54:**79–88.
13. **Casalegno, J. S., et al.** 2010. Oseltamivir-resistant influenza A(H1N1) viruses in south of France, 2007/2009. Antiviral Res. [Epub ahead of print.] doi:10.1016/j.antiviral.2010.05.010.
14. **Chong, A. K., M. S. Pegg, N. R. Taylor, and M. von Itzstein.** 1992. Evidence for a sialosyl cation transition-state complex in the reaction of sialidase from influenza virus. Eur. J. Biochem. **207:**335–343.
15. **Colman, P. M., P. A. Hoyne, and M. C. Lawrence.** 1993. Sequence and structure alignment of paramyxovirus hemagglutinin-neuraminidase with influenza virus neuraminidase. J. Virol. **67:**2972–2980.
16. **Colman, P. M., J. N. Varghese, and W. G. Laver.** 1983. Structure of the catalytic and antigenic sites in influenza virus neuraminidase. Nature **303:**41–44.
17. **Dharan, N. J., et al.** 2009. Infections with oseltamivir-resistant influenza A(H1N1) virus in the United States. JAMA **301:**1034–1041.
18. **Escuret, V., et al.** 2008. Detection of human influenza A (H1N1) and B strains with reduced sensitivity to neuraminidase inhibitors. J. Clin. Virol. **41:**25–28.
19. **Ferraris, O., N. Kessler, and B. Lina.** 2005. Sensitivity of influenza viruses to zanamivir and oseltamivir: a study performed on viruses circulating in France prior to the introduction of neuraminidase inhibitors in clinical practice. Antiviral Res. **68:**43–48.
20. **Ferraris, O., and B. Lina.** 2008. Mutations of neuraminidase implicated in neuraminidase inhibitors resistance. J. Clin. Virol. **41:**13–19.
21. **Gubareva, L. V.** 2004. Molecular mechanisms of influenza virus resistance to neuraminidase inhibitors. Virus Res. **103:**199–203.
22. **Gubareva, L. V., et al.** 1996. Characterization of mutants of influenza A virus selected with the neuraminidase inhibitor 4-guanidino-Neu5Ac2en. J. Virol. **70:**1818–1827.
23. **Gubareva, L. V., L. Kaiser, M. N. Matrosovich, Y. Soo-Hoo, and F. G. Hayden.** 2001. Selection of influenza virus mutants in experimentally infected volunteers treated with oseltamivir. J. Infect. Dis. **183:**523–531.
24. **Gubareva, L. V., M. J. Robinson, R. C. Bethell, and R. G. Webster.** 1997. Catalytic and framework mutations in the neuraminidase active site of influenza viruses that are resistant to 4-guanidino-Neu5Ac2en. J. Virol. **71:**3385–3390.
25. **Hatakeyama, S., et al.** 2007. Emergence of influenza B viruses with reduced sensitivity to neuraminidase inhibitors. JAMA **297:**1435–1442.
26. **Herlocher, M. L., et al.** 2002. Influenza virus carrying an R292K mutation in the neuraminidase gene is not transmitted in ferrets. Antiviral Res. **54:**99–111.
27. **Herlocher, M. L., et al.** 2004. Influenza viruses resistant to the antiviral drug oseltamivir: transmission studies in ferrets. J. Infect. Dis. **190:**1627–1630.
28. **Hoffmann, E., G. Neumann, Y. Kawaoka, G. Hobom, and R. G. Webster.** 2000. A DNA transfection system for generation of influenza A virus from eight plasmids. Proc. Natl. Acad. Sci. U. S. A. **97:**6108–6113.
29. **Hurt, A. C., I. G. Barr, G. Hartel, and A. W. Hampson.** 2004. Susceptibility of human influenza viruses from Australasia and South East Asia to the neuraminidase inhibitors zanamivir and oseltamivir. Antiviral Res. **62:**37–45.
30. **Hurt, A. C., et al.** 2009. Emergence and spread of oseltamivir-resistant A(H1N1) influenza viruses in Oceania, South East Asia and South Africa. Antiviral Res. **83:**90–93.
31. **Hurt, A. C., J. K. Holien, and I. G. Barr.** 2009. In vitro generation of neuraminidase inhibitor resistance in A(H5N1) influenza viruses. Antimicrob. Agents Chemother. **53:**4433–4440.
32. **Jackson, D., W. Barclay, and T. Zurcher.** 2005. Characterization of recombinant influenza B viruses with key neuraminidase inhibitor resistance mutations. J. Antimicrob. Chemother. **55:**162–169.
33. **Kim, C. U., et al.** 1997. Influenza neuraminidase inhibitors possessing a novel hydrophobic interaction in the enzyme active site: design, synthesis, and structural analysis of carbocyclic sialic acid analogues with potent anti-influenza activity. J. Am. Chem. Soc. **119:**681–690.
34. **Kiso, M., et al.** 2004. Resistant influenza A viruses in children treated with oseltamivir: descriptive study. Lancet **364:**759–765.
35. **Li, W., et al.** 1998. Identification of GS 4104 as an orally bioavailable prodrug of the influenza virus neuraminidase inhibitor GS 4071. Antimicrob. Agents Chemother. **42:**647–653.
36. **Liu, C., M. C. Eichelberger, R. W. Compans, and G. M. Air.** 1995. Influenza type A virus neuraminidase does not play a role in viral entry, replication, assembly, or budding. J. Virol. **69:**1099–1106.
37. **Lowen, A. C., S. Mubareka, T. M. Tumpey, A. Garcia-Sastre, and P. Palese.** 2006. The guinea pig as a transmission model for human influenza viruses. Proc. Natl. Acad. Sci. U. S. A. **103:**9988–9992.
38. **Matrosovich, M., T. Matrosovich, J. Carr, N. A. Roberts, and H. D. Klenk.** 2003. Overexpression of the alpha-2,6-sialyltransferase in MDCK cells increases influenza virus sensitivity to neuraminidase inhibitors. J. Virol. **77:**8418–8425.
39. **Meijer, A., et al.** 2009. Oseltamivir-resistant influenza virus A (H1N1), Europe, 2007-08 season. Emerg. Infect. Dis. **15:**552–560.
40. **Mishin, V. P., F. G. Hayden, and L. V. Gubareva.** 2005. Susceptibilities of antiviral-resistant influenza viruses to novel neuraminidase inhibitors. Antimicrob. Agents Chemother. **49:**4515–4520.
41. **Monto, A. S., et al.** 2006. Detection of influenza viruses resistant to neuraminidase inhibitors in global surveillance during the first 3 years of their use. Antimicrob. Agents Chemother. **50:**2395–2402.
42. **Moules, V., et al.** 2010. In vitro characterization of naturally occurring influenza H3NA- viruses lacking the NA gene segment: toward a new mechanism of viral resistance? Virology **404:**215–224.
43. **Okomo-Adhiambo, M., et al.** 2010. Detection of E119V and E119I mutations in influenza A (H3N2) viruses isolated from an immunocompromised patient: challenges in diagnosis of oseltamivir resistance. Antimicrob. Agents Chemother. **54:**1834–1841.
44. **Palese, P., and R. W. Compans.** 1976. Inhibition of influenza virus replication in tissue culture by 2-deoxy-2,3-dehydro-N-trifluoroacetylneuraminic acid (FANA): mechanism of action. J. Gen. Virol. **33:**159–163.

45. **Palese, P., K. Tobita, M. Ueda, and R. W. Compans.** 1974. Characterization of temperature sensitive influenza virus mutants defective in neuraminidase. Virology **61:**397–410.

46. **Rameix-Welti, M. A., et al.** 2006. Natural variation can significantly alter the sensitivity of influenza A (H5N1) viruses to oseltamivir. Antimicrob. Agents Chemother. **50:**3809–3815.

47. **Rameix-Welti, M. A., V. Enouf, F. Cuvelier, P. Jeannin, and S. van der Werf.** 2008. Enzymatic properties of the neuraminidase of seasonal H1N1 influenza viruses provide insights for the emergence of natural resistance to oseltamivir. PLoS Pathog. **4:**e1000103.

48. **Reed, L. J., and H. Muench.** 1938. A simple method of estimating fifty percent endpoints. Am. J. Hyg. **27:**493–497.

49. **Richard, M., et al.** 2008. Impact of influenza A virus neuraminidase mutations on the stability, activity, and sensibility of the neuraminidase to neuraminidase inhibitors. J. Clin. Virol. **41:**20–24.

50. **Rudrawar, S., et al.** 2010. Novel sialic acid derivatives lock open the 150-loop of an influenza A virus group-1 sialidase. Nat. Commun. **1:**113.

51. **Russell, R. J., et al.** 2006. The structure of H5N1 avian influenza neuraminidase suggests new opportunities for drug design. Nature **443:**45–49.

52. **Sauter, N. K., et al.** 1989. Hemagglutinins from two influenza virus variants bind to sialic acid derivatives with millimolar dissociation constants: a 500-MHz proton nuclear magnetic resonance study. Biochemistry **28:**8388–8396.

53. **Sheu, T. G., et al.** 2008. Surveillance for neuraminidase inhibitor resistance among human influenza A and B viruses circulating worldwide from 2004 to 2008. Antimicrob. Agents Chemother. **52:**3284–3292.

54. **Tai, C. Y., et al.** 1998. Characterization of human influenza virus variants selected in vitro in the presence of the neuraminidase inhibitor GS 4071. Antimicrob. Agents Chemother. **42:**3234–3241.

55. **Tashiro, M., et al.** 2009. Surveillance for neuraminidase-inhibitor-resistant influenza viruses in Japan, 1996-2007. Antivir. Ther. **14:**751–761.

56. **Taylor, N. R., and M. von Itzstein.** 1994. Molecular modeling studies on ligand binding to sialidase from influenza virus and the mechanism of catalysis. J. Med. Chem. **37:**616–624.

57. **Tulip, W. R., et al.** 1991. Refined atomic structures of N9 subtype influenza virus neuraminidase and escape mutants. J. Mol. Biol. **221:**487–497.

58. **Varghese, J. N., and P. M. Colman.** 1991. Three-dimensional structure of the neuraminidase of influenza virus A/Tokyo/3/67 at 2.2 A resolution. J. Mol. Biol. **221:**473–486.

59. **Varghese, J. N., W. G. Laver, and P. M. Colman.** 1983. Structure of the influenza virus glycoprotein antigen neuraminidase at 2.9 A resolution. Nature **303:**35–40.

60. **Varghese, J. N., J. L. McKimm-Breschkin, J. B. Caldwell, A. A. Kortt, and P. M. Colman.** 1992. The structure of the complex between influenza virus neuraminidase and sialic acid, the viral receptor. Proteins **14:**327–332.

61. **von Itzstein, M., et al.** 1993. Rational design of potent sialidase-based inhibitors of influenza virus replication. Nature **363:**418–423.

62. **Wang, M. Z., C. Y. Tai, and D. B. Mendel.** 2002. Mechanism by which mutations at His274 alter sensitivity of influenza A virus N1 neuraminidase to oseltamivir carboxylate and zanamivir. Antimicrob. Agents Chemother. **46:**3809–3816.

63. **Wetherall, N. T., et al.** 2003. Evaluation of neuraminidase enzyme assays using different substrates to measure susceptibility of influenza virus clinical isolates to neuraminidase inhibitors: report of the neuraminidase inhibitor susceptibility network. J. Clin. Microbiol. **41:**742–750.

64. **Yen, H. L., et al.** 2005. Neuraminidase inhibitor-resistant influenza viruses may differ substantially in fitness and transmissibility. Antimicrob. Agents Chemother. **49:**4075–4084.

65. **Yen, H. L., et al.** 2006. Importance of neuraminidase active-site residues to the neuraminidase inhibitor resistance of influenza viruses. J. Virol. **80:**8787–8795.

66. **Yen, H. L., et al.** 2007. Inefficient transmission of H5N1 influenza viruses in a ferret contact model. J. Virol. **81:**6890–6898.